

Article

Mechanical and Tribological Study on Aluminum Coatings with High-Pressure and Low-Pressure Cold-Spray Processes

Abreeza Manap ^{1,2,*} , NF Afandi ¹, Savisha Mahalingam ² , Siti Nurul Akmal Yusof ³ and Zulkifli Mohd. Rosli ⁴¹ College of Engineering, Universiti Tenaga Nasional, Jalan IKRAM-UNITEN, Kajang 43000, Selangor, Malaysia² Institute of Sustainable Energy, Universiti Tenaga Nasional, Jalan IKRAM-UNITEN, Kajang 43000, Selangor, Malaysia³ Department of Mechanical Precision Engineering, Malaysia-Japan International Institute of Technology, Universiti Teknologi Malaysia, Jalan Sultan Yahya Petra, Kuala Lumpur 54100, Selangor, Malaysia⁴ Fakulti Teknologi Kejuruteraan Mekanikal Dan Pembuatan, Universiti Teknikal Malaysia Melaka, Hang Tuah Jaya, Durian Tunggal 76100, Melaka, Malaysia

* Correspondence: abreeza@uniten.edu.my; Tel.: +60-3-89212020 (ext. 7310)

Abstract: Cold spray is a promising approach to repair all damages and defects in aluminum (Al) constituent elements. The study aims to investigate the mechanical and tribological properties of Al coatings deposited using high-pressure cold-spray (HPCS) and low-pressure cold-spray (LPCS) techniques. Al powder was sprayed on a cold-rolled plate of aluminum 1100, which was used as the substrate. The results showed that the micro-hardness of the LPCS Al coating reached up to 196.6 HV before the wear test compared to that of HPCS (174.3 HV). Moreover, more low friction coefficients obtained by LPCS (0.798) than HPCS (0.807) indicated good tribological properties with a high amount of oxide composition. Meanwhile, the wear studies reveal that the specific wear rate of the Al coating of LPCS (0.008) was lower than the HPCS (0.009) as the load increased from 3 N to 5 N, thus providing excellent wear resistance. Therefore, the results exhibited greater mechanical and tribological characteristics for Al coatings produced by the LPCS process than by the HPCS process.

Keywords: energy; friction coefficient; high-pressure cold spray; low-pressure cold spray; specific wear rate



Citation: Manap, A.; Afandi, N.; Mahalingam, S.; Yusof, S.N.A.; Mohd. Rosli, Z. Mechanical and Tribological Study on Aluminum Coatings with High-Pressure and Low-Pressure Cold-Spray Processes. *Coatings* **2022**, *12*, 1792. <https://doi.org/10.3390/coatings12111792>

Academic Editor: Jose Ygnacio Pastor

Received: 21 October 2022

Accepted: 17 November 2022

Published: 21 November 2022

Publisher's Note: MDPI stays neutral with regard to jurisdictional claims in published maps and institutional affiliations.



Copyright: © 2022 by the authors. Licensee MDPI, Basel, Switzerland. This article is an open access article distributed under the terms and conditions of the Creative Commons Attribution (CC BY) license (<https://creativecommons.org/licenses/by/4.0/>).

1. Introduction

Aluminum (Al) alloys are lightweight, non-ferrous metal with high corrosion resistance [1,2] and ductility. The high strength of Al provides reduces fuel consumption in transportation systems such as aircraft, railcars, and light vehicles. Furthermore, it is known as an excellent electric conductor [3]; Al wire is used for transmitting electrical power over long distances. It also has the potential to be used in heat exchangers, refrigerators, and air conditioners because of its good thermal-conductor properties. However, damages may occur in Al components that cannot be repaired with conventional technologies [1]. For instance, bores in the Al castings are subject to damages such as corrosion and wear. Corrosion takes place as Al components are readily oxidized, including when Al is present either in solid solution or intermetallic particles. Welding Al components is difficult because of its high specific thermal conductivity and high coefficient of thermal expansion [1,4].

Within the last decade, numerous studies have been carried out to investigate the wear performance of metal coatings produced by thermal spray, including high-velocity oxy-fuel, combustion flame, vacuum plasma, and two-wire electric arc [5]. Even though these thermal-spray processes use strong and clean spraying methods, the heat dissipation may change the microstructure of the coatings and their mechanical behavior, leading to coating particle oxidation, decomposition, and grain growth, which is a major threat in coating technology [6,7]. In order to overcome these damages, cold spray (CS) can be utilized as a new approach in the coating technique. The main benefit of CS over thermal

spray techniques is that the coating material is not thermally altered. This event minimizes any possible phase transformation and sustains the particles in their unmodified solid state.

There are two types of CS methods: high-pressure cold spray (HPCS) and low-pressure cold spray (LPCS). The HPCS process used helium or nitrogen as working gas, at high pressure (2.0–4.0 MPa), and preheated it (up to 1000 °C) inside the de Laval type nozzle [8–11]. The particle velocities for this process range from 200 to 1200 m/s [12], which allows for the deposition of various materials ranging from pure metal to alloys. A study on Al coatings deposited using HPCS has been reported extensively by several researchers [9–15]. Efficient bonding for Al coating occurs between 600 and 900 m/s, within which the highest deposition efficiency can be achieved [9–13]. However, the mechanical properties of Al coating deposited using HPCS were unsatisfactory. Some particles did not severely deform, which resulted in lower hardness and high coating porosity [16–18]. A similar outcome was also reported for other light materials. The examination of these light-metal coatings revealed a decrease in hardness with increasing distance from the substrate, despite displaying excellent impact behaviors such as severe plastic deformation in the substrate, intimate metallurgical (atomic) bond-forming along the interface, and an increase in hardness at the interface region as a result of grain refinement [19–21]. Thus, HPCS is deemed as not suitable for depositing soft and light materials [22].

The LPCS process used compressed gas as a working gas at relatively low pressure (below 0.6 MPa) and preheated it (up to 550 °C) inside the de Laval type nozzle [8–10]. The particle velocities for LPCS range from 350 to 700 m/s [23]. The velocity for depositing Al using LPCS ranges from 300 to 500 ms⁻¹ [11–14]. Due to the relatively lower velocity of LPCS, it is believed that erosion on the Al substrate surface can be avoided. Despite the potential exhibited by the LPCS method, the impact behavior of light metals, including Al, has not been sufficiently investigated using this technique. In our previous work, computer simulation was used to investigate Al particle impact on the Al substrate during HPCS and LPCS coating processes [16]. It was found that Al deposited using LPCS resulted in lower porosity than Al deposited using HPCS. Therefore, it is of great importance to extend the study and investigate the coating properties as well as the tribological properties.

Moreover, there is no study comparing HPCS and LPCS methods with Al deposition in a single work. Therefore, the present work aims to investigate the mechanical and tribological properties of Al coatings deposited using HPCS and LPCS. Several analyses were conducted by evaluating the different coating spray processes' microstructure, elemental composition, hardness, wear rate, friction of coefficient, and wear resistance.

2. Materials and Methods

2.1. Cold-Spray Deposition Process

The HPCS and LPCS coatings were produced by PCS-203 (Plasma Giken Kogyo Co., Ltd., Saitama, Japan) and DYMET403J (Obninsk Center for Powder Spraying, Kaluga Oblast, Russia), respectively. Figure 1 shows the schematic diagram of the HPCS and LPCS system with the spraying parameters, as listed in Table 1. The spray material (pure Al powder of AL G-AT; particle diameter: 25 µm) was purchased from Fukuda Metal Foil and Powder Corporation (Kyoto, Japan). A cold-rolled plate of aluminum 1100 was used as the substrate. Helium and compressed air were used as the carrier gas for HPCS (2.0 MPa) and LPCS (0.6 MPa), respectively. The temperature was set up at 300 K with a nozzle distance of 15 mm.

2.2. Mechanical and Wear Test

The hardness of the different coating processes was measured using the Vickers hardness test machine (Hitachi, Universiti Tenaga Nasional, Selangor, Malaysia). The test was conducted at room temperature (30 °C), and the measurement of hardness was taken at three different places on each sample to obtain the average value of hardness. The pore size was analyzed using the image analysis method. Friction and wear tests were performed with micro pin-on-disc tribotester (model CM-9109, Ducom, Bangalore, India) according to

the G99 ASTM standard test method. The pin-on-disc tribotester schematic is illustrated in Figure 2. Wear test samples were placed inside the steel pin holder, which was 15 mm in diameter. The test surface and wear-disc holder were cleaned with soft cotton after each run on the machine to remove any wear debris. The sliding tests were performed on a wear track diameter of 30 mm for a constant sliding distance of 400 m under ambient conditions. The tests were conducted for different loads (2 N, 3 N, and 5 N) and a sliding velocity constant at 0.1 m/s. The wear-test parameters are given in Table 2.

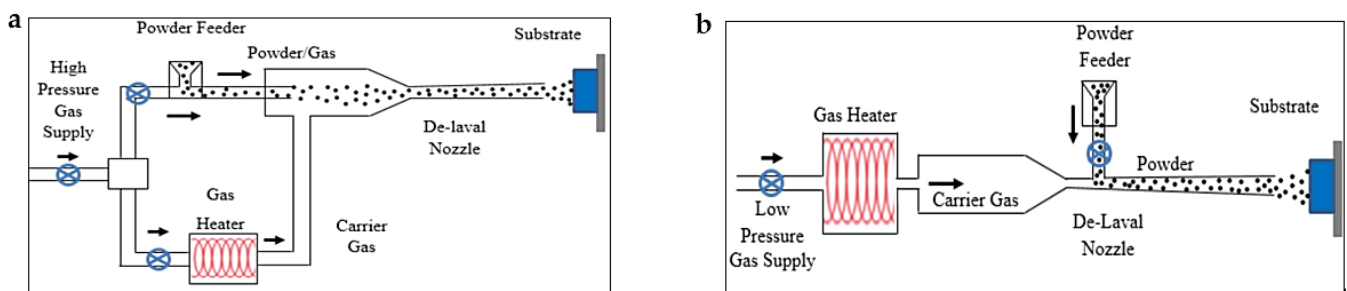


Figure 1. Schematic diagram of (a) HPCS and (b) LPCS [24].

Table 1. Spraying parameters of HPCS and LPCS.

Parameters	HPCS	LPCS
Size (μm)	25	25
Working gas	Helium	Air
Gas pressure (MPa)	2.0	0.6
Initial temperature (K)	300	300
Nozzle distance (mm)	15	15
Number of layers	20	20

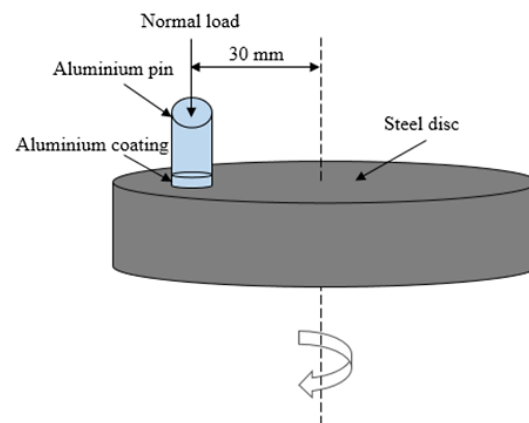


Figure 2. Schematic diagram of micro pin-on-disc tribotester.

Table 2. Wear-test parameters.

Parameters	Selected Value
Applied load (N)	2, 3 and 5
Velocity (m/s)	0.1
Environment	Air
Temperature ($^{\circ}\text{C}$)	25 ± 2
Humidity (%)	55 ± 5
Speed of motor (rpm)	200
Sliding distance (m)	400
Track diameter (mm)	30
Duration (s)	960

2.3. Characterization

The samples were cut using the Buehler Isomet Precision Saw. The cutter speed was set to a low-speed setting, which is 100 rpm. Then, the samples were mounted using the cold mounting technique. The mounting materials used were resin from Struers Epoxy kit that included epoxy resin and epoxy hardener. In order to obtain a highly reflective surface that was free from scratches and deformation, the samples had to be carefully ground and polished before they could be examined under the microscope. The samples were ground using silicon carbide papers of 800 and 1000 grit sizes and followed by a polishing process using a diamond solution as the polisher. The cross-sectional microstructures, surface morphologies, and wear tracks were examined using scanning electron microscopy (SEM) (Hitachi SU1510, Tokyo, Japan). The elemental composition of the coating and the substrate were determined using energy-dispersive X-ray spectroscopy (EDX) (Hitachi SU1510, Tokyo, Japan).

3. Results

3.1. Microstructure and Mechanical

The microstructure images of Al coatings deposited using HPCS and LPCS are shown in Figure 3. According to visual examination from Figure 3a, pores indicated by the arrow show that HPCS coating exhibited larger pores between the particles compared to that of LPCS in Figure 3b. To confirm this observation, the pore-size distribution was plotted and quantified using a histogram, as shown in Figure 4. The average pore size of the HPCS coating is approximately 0.35 μm , and the average pore size of the LPCS coating is approximately 0.18 μm .

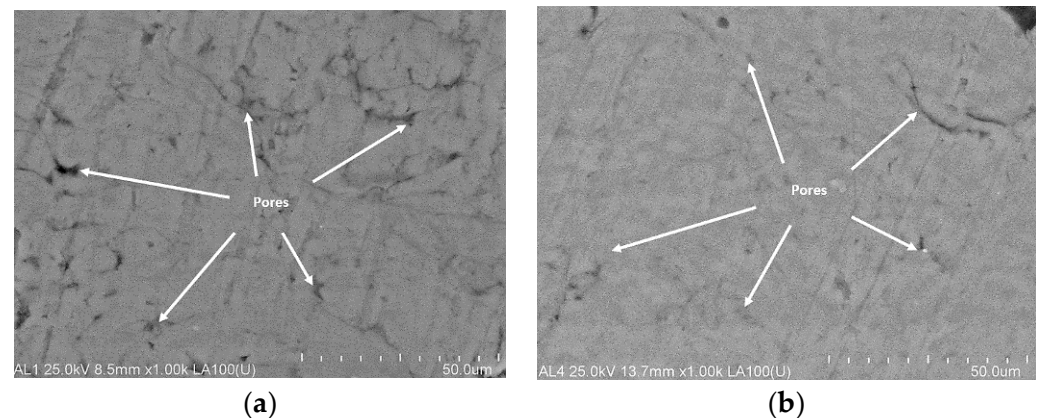


Figure 3. SEM images of Al coatings using (a) HPCS and (b) LPCS.

Smaller average pore size is obtained in the LPCS coating due to the full deformation of the sprayed Al particles that leads to good bonding between the sprayed particles and the substrate. Furthermore, the smaller pore-size distribution in the LPCS coating contributes to denser coating with lower porosity. The porosity of the Al coatings deposited using HPCS and LPCS on Al substrates is given in Table 3. It is the measure of pore area over total area. The LPCS coating has lower porosity (3.48%) than the HPCS coating (7.72%). A previous study in [17] claimed that high porosity in Al coatings reduces the mechanical properties where porosity is one of the key factors that influences the mechanical and wear performance in coatings. Hence, it is inferred that the lower porosity observed in LPCS coating could improve the mechanical and wear performances, which can be assessed through microhardness, friction, and wear tests.

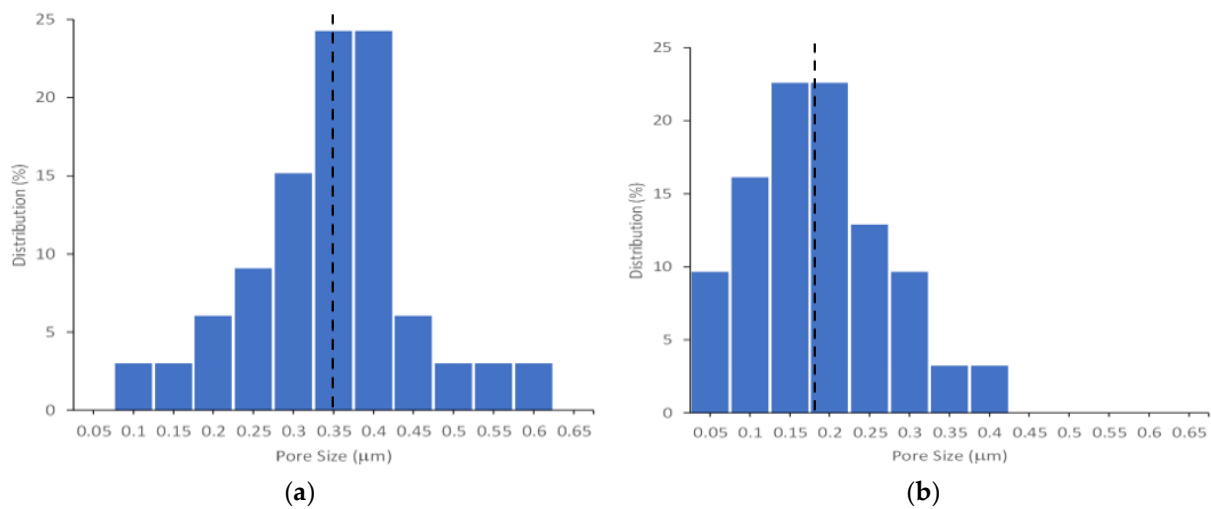


Figure 4. Pore size distribution of Al coatings using (a) HPCS and (b) LPCS. (Dotted line is average pore size, for (a) 0.35 micrometer and (b) 0.18 micrometer).

Table 3. Vickers hardness and porosity of HPCS and LPCS coatings.

Process	Vickers Hardness (HV)	Porosity (%)
HPCS	174.3	7.72
LPCS	196.6	3.48

The microhardness obtained through the Vickers Hardness test of Al coatings deposited using HPCS and LPCS on Al substrates is also summarized in Table 3. The LPCS coating has a higher hardness of 196.6 HV than the HPCS coating, which is 174.3 HV. This is attributed to the lower porosity of the LPCS coating. According to Lee et al., the Al coating deposited using LPCS has higher hardness due to the peening effect from the low coating porosity [18].

Higher hardness indicates work-hardening resulting from plastic deformation and strain-hardening during particle impacts [18], which can be easily achieved using HPCS through the severe deformation of the particles on the substrate. However, the presence of larger pores in the HPCS-sprayed Al coating is due to the peculiarities of the HPCS process on lightweight materials. Although the first layer of particles was fully deformed, the continuous bombardment of subsequent particles at high velocity resulted in large pores between the particles. These large pores prevent the formation of compact and coherent layers. On the other hand, the smaller pores formed between the Al particles through the LPCS result in a dense coating. Therefore, the LPCS induces a high level of plastic deformation on the Al coating, as well as strain hardening, which in turn increases hardness in the coating.

3.2. Friction and Wear

Wear, and friction, tests were performed on a pin-on-disc wear-test machine. Figure 5 shows the wear load and frictional force of HPCS and LPCS coatings as a function of time under 2 N, which are used to calculate the wear rate and the specific wear rate. The wear rate and specific wear rate are given as in the following equation:

$$\dot{W} = \frac{v}{F_n d} \quad (1)$$

$$\dot{V} = K\dot{W} \quad (2)$$

where \dot{W} is the specific wear rate, which is simply the wear volume v divided by the product of the normal load F_n and the sliding distance d . Moreover, \dot{V} is the wear rate and K is the wear constant.

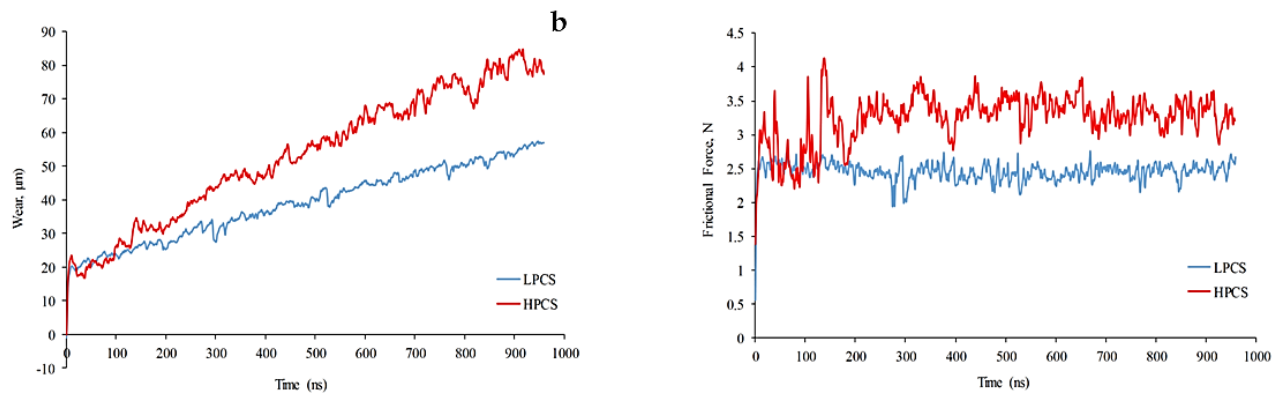


Figure 5. (a) Wear load; (b) frictional force of Al coatings using HPCS and LPCS.

Figure 6 shows the variation of the friction coefficient of Al coating deposited using HPCS and LPCS as a function of time subjected to 2 N. The wear tests conducted on the HPCS and LPCS coatings demonstrated that the friction coefficient varied between 0.001 and 1.8 μ and between 0.3 and 1.4 μ for HPCS and LPCS, respectively, as seen in Figure 6. These results show that the LPCS coating has a smaller range of friction coefficient than the HPCS coating.

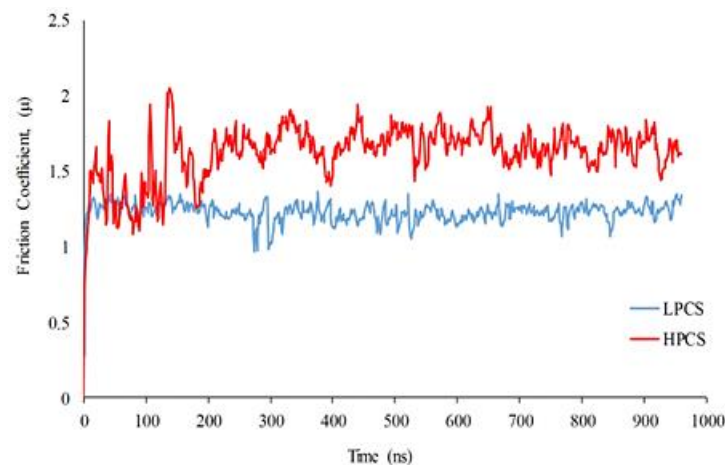


Figure 6. Friction coefficient at 2 N load of Al coatings using HPCS and LPCS.

Furthermore, Figure 7a,b demonstrate the variation of friction coefficients and the wear rate of Al coatings as a function of applied load (2 N, 3 N, and 5 N) deposited using HPCS and LPCS, respectively. The friction coefficient for both the HPCS and LPCS coatings decreases as the load increases from 2 N to 5 N. This shows that CS technology decreases the friction coefficient [22]. Comparing the HPCS and LPCS coatings, the friction coefficient of the LPCS coating decreased gradually from 1.343 to 1.297 and then to 0.798 with small gaps in the values as the load was increased, whereas the HPCS coating decreased from 1.609 to 1.067 and then to 0.807 with larger gaps. As stated in [22], dense coatings with low porosity generate a low friction coefficient that improves wear resistance.

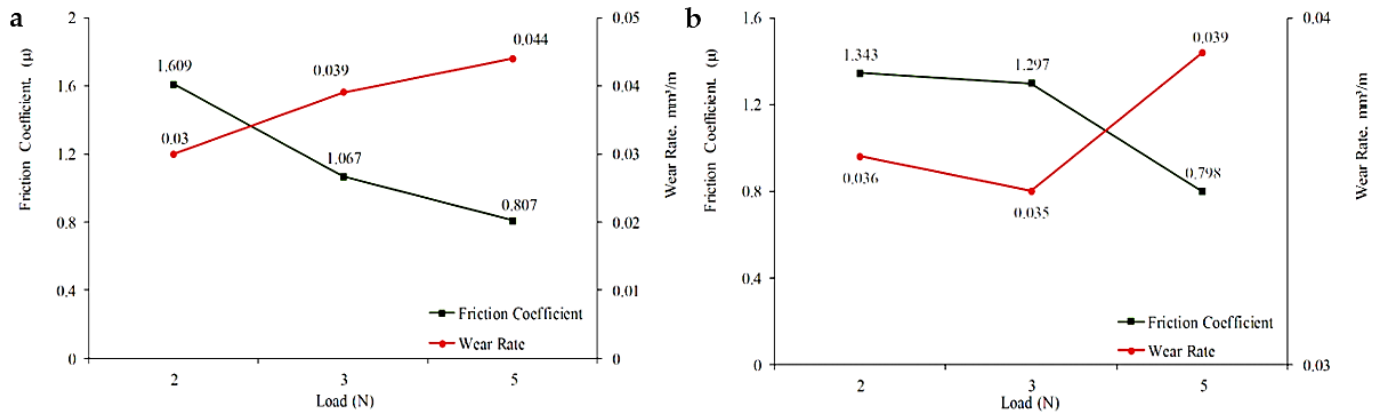


Figure 7. Friction coefficient and wear rate at 2, 3, and 5 N loads of Al coatings using (a) HPCS and (b) LPCS.

However, the wear rate increased for both HPCS and LPCS coatings as the load increased from 2 N to 5 N, as seen in Figure 7. This is because the wear rate is independent of the applied load, as observed in Equation (2). Figure 8a,b show the specific wear rate and wear resistance of Al coatings as a function of applied load (2 N, 3 N, and 5 N) deposited using HPCS and LPCS, respectively. The specific wear rate decreased for both HPCS and LPCS coatings as the applied load increased. Even though the specific wear rate of LPCS coating (0.016 mm³/Nm) was higher than the HPCS coating (0.015 mm³/Nm) at the low load of 2 N, the specific wear rate of the LPCS coating decreased as the load was increased to 5 N. The lower specific wear rate of the LPCS coating at a higher applied load led to a higher value of wear resistance (98.5 Nm/mm³) than the HPCS coating (98.2 Nm/mm³).

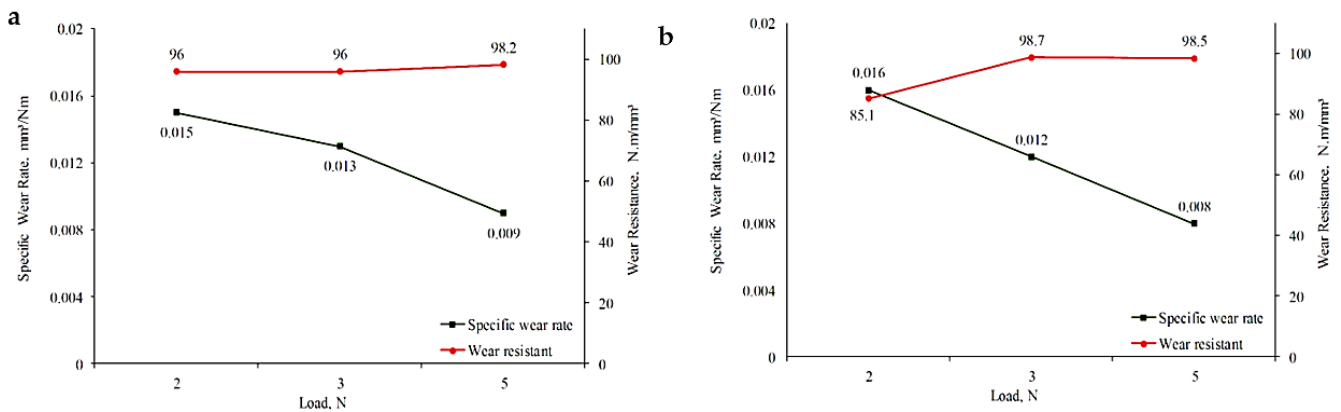


Figure 8. Specific wear rate and wear resistance at 2, 3, and 5 N loads of Al coatings using (a) HPCS and (b) LPCS.

Figures 9 and 10 show the SEM images of wear tracks subjected to different loads of 2 N, 3 N, and 5 N, formed on HPCS and LPCS coatings, respectively. The wear track on the HPCS coating shows a smoother surface with only small patches and grooves in the 2 N load compared to the 3 N and 5 N loads. The wear tracks on higher loads (3 N and 5 N) have more patches with deep grooves. On the other hand, the wear track on the LPCS coating with a low load of 2 N provides a regular surface profile with a small number of cracks and cavities (Figure 10a). The wear track with 3 N of the applied load demonstrates grooves on the surface (Figure 10b).

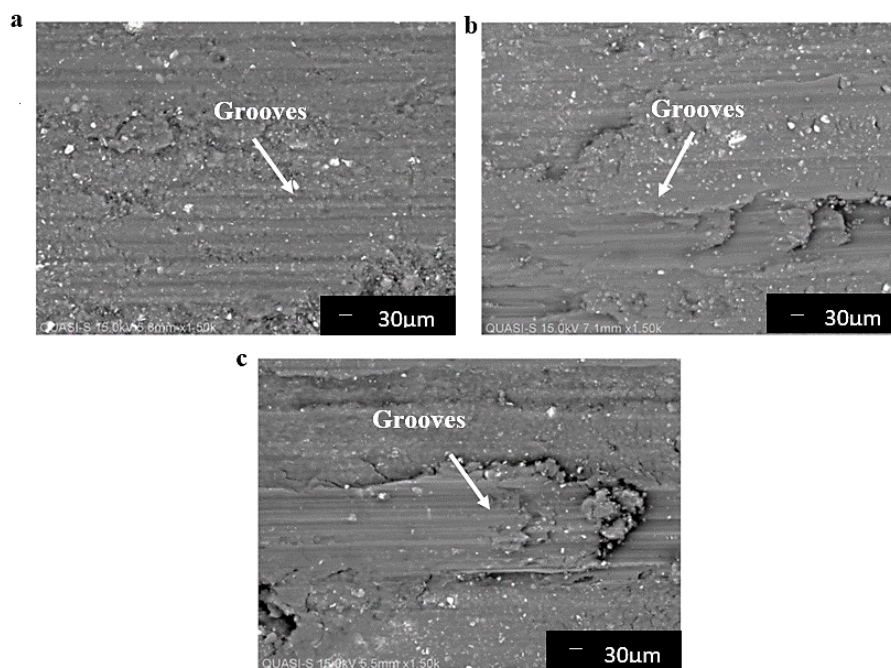


Figure 9. SEM image of HPCS Al coatings at an applied loads of (a) 2 N; (b) 3 N; and (c) 5 N.

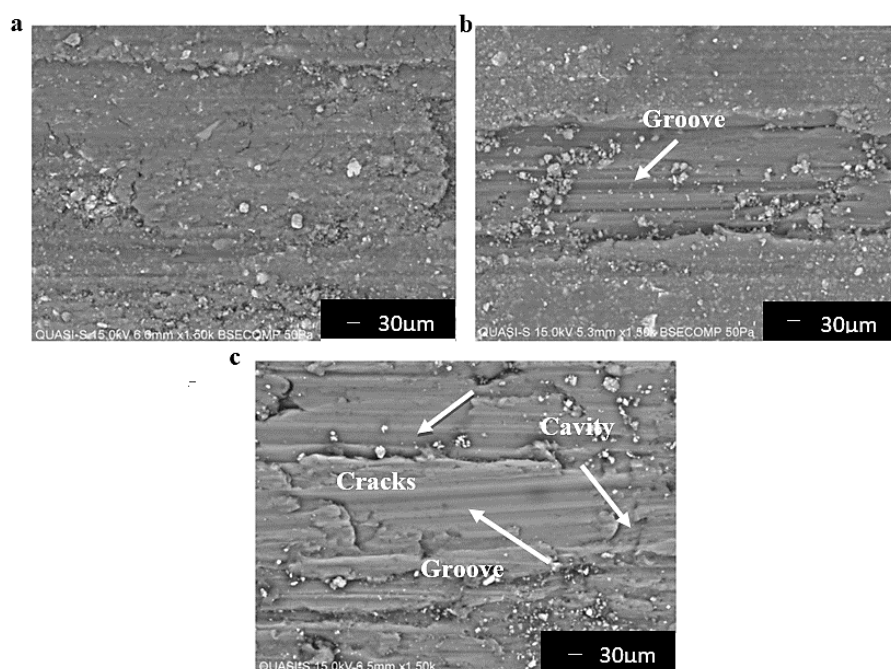


Figure 10. SEM image of LPCS Al coatings at an applied load of (a) 2 N; (b) 3 N; and (c) 5 N.

In contrast, the wear track with the 5 N load shows the formation of larger cracks, small cavities, and grooves on the surface (Figure 10c). The composition of oxygen in the HPCS and LPCS coatings is tabulated in Table 4. The results show that the composition of oxygen increases as the load increases for both the HPCS and the LPCS coating. The LPCS coating, however, exhibits a higher amount of oxygen with increasing load. This may contribute to its low friction coefficient observed in Figure 7b.

Table 4. EDX result of HPCS and LPCS.

Process	Oxygen Composition (%)			
	Initial	2 N	3 N	5 N
HPCS	16.49	17.02	31.20	45.38
LPCS	18.85	16.59	35.23	47.18

According to Asuke et al. [25], the wear rate increases with increasing applied load because the amount of wear loss is small when a small load is applied. Besides that, the drastic reduction in specific wear rate for HPCS and LPCS coatings from 0.015 mm³/Nm to 0.009 mm³/Nm (Figure 8a) and from 0.016 mm³/Nm to 0.008 mm³/Nm (Figure 8b), respectively, is due to the effectiveness of the oxide layer formed on the surface. Stott mentioned that the high oxide layer formed on the surface of the coating contributes to a low specific wear rate [26,27]. The lower specific wear rate exhibited by the LPCS coating at higher loads (3 N and 5 N) than the HPCS coating indicates that the oxide layer inhibits contact between the surfaces, which may improve the wear resistance in the coating. Accordingly, the LPCS coating showed more excellent wear resistance at higher applied loads of 3 N and 5 N, with a high amount of oxygen composition of 35.23% and 47.18%, respectively, whereby high wear resistance indicates improved wear resistance and, therefore, good tribological properties [25].

The obtained results depict that the worn surfaces on the wear track of the HPCS and LPCS coatings denote the presence of an oxide layer resulting from the formation of cracks and cavities. This oxide layer, which is formed by oxidative wear, protects the Al coating from wear when it is in contact with a counter-face and induces low friction. One reason for the low friction is the formation of low-strength microfilms, in this case the growth of aluminum oxide (Al₂O₃) between the contacting surfaces. Therefore, the high amount of oxygen (47.18%) in the LPCS coating subjected to the 5 N load contributes to the large cracks and small cavities formed on the worn surfaces, as observed in Figure 10c. Moreover, the formation of an oxide layer leads to a low friction coefficient, as observed in Figure 7. Therefore, due to the higher amount of oxygen composition in the LPCS coating, the Al coating deposited using LPCS exhibits better wear properties than that of HPCS.

4. Conclusions

In summary, the mechanical and tribological properties of Al coatings using the HPCS and LPCS processes were successfully studied. The micro-hardness of the Al coating using the LPCS process before the wear test reached up to 196.6 HV, which is higher than the Al coating using the HPCS process (174.3 HV). Meanwhile, the pore size increases with increasing porosity, which influences the mechanical and wear performance. Al coating using the LPCS process has a lower percentage of pore-size diameter than the HPCS process. The lower percentage of pore diameter contributes to a dense coating with less porosity. Moreover, the low friction coefficients obtained by the LPCS process indicate the good tribological properties of the Al coating, with a high amount of oxide composition. The wear studies reveal that the specific wear rate of Al coating using the LPCS process is lower as the load increases from 3 N to 5 N, thus providing greater wear resistance than that of the HPCS coating.

Author Contributions: Conceptualization, A.M. and S.N.A.Y.; methodology, A.M. and S.N.A.Y.; software, A.M., N.A., and S.N.A.Y.; validation, A.M. and S.N.A.Y.; formal analysis, S.N.A.Y.; investigation, S.N.A.Y.; resources, A.M.; data curation, S.N.A.Y.; writing—original draft preparation, S.M. and S.N.A.Y.; writing—review and editing, A.M., N.A., S.M., S.N.A.Y. and Z.M.R.; visualization, N.A. and Z.M.R.; supervision, A.M.; project administration, A.M.; and funding acquisition, A.M. All authors have read and agreed to the published version of the manuscript.

Funding: This research was funded by the Ministry of Higher Education Malaysia (MoHE) and the Universiti Tenaga Nasional (UNITEN) for funding this study under the fundamental research-grant scheme (FRGS) of Grant No. 20130108FRGS, and the APC was funded by UNITEN, Grant No. Grant No. J510050002—IC-6 BOLDREFRESH2025—CENTRE OF EXCELLENCE.

Institutional Review Board Statement: Not applicable.

Informed Consent Statement: Not applicable.

Data Availability Statement: Not applicable.

Acknowledgments: The authors would like to thank the Ministry of Higher Education Malaysia (MoHE) and Universiti Tenaga Nasional (UNITEN) for funding this study under the fundamental research-grant scheme (FRGS) of Grant No. 20130108FRGS.

Conflicts of Interest: The authors declare no conflict of interest.

References

1. Ogawa, K.; Ito, K.; Ichimura, K.; Ichikawa, Y.; Ohno, S.; Onda, N. Characterization of low-pressure cold-sprayed aluminum coatings. *J. Therm. Spray Technol.* **2000**, *17*, 728–735. [\[CrossRef\]](#)
2. Nordheim, E.; Barrasso, G. Sustainable development indicators of the European aluminium industry. *J. Clean. Prod.* **2007**, *15*, 275–279. [\[CrossRef\]](#)
3. Wang, G.; Zhang, L.; Zhang, J. A review of electrode materials for electrochemical supercapacitors. *Chem. Soc. Rev.* **2012**, *41*, 797–828. [\[CrossRef\]](#) [\[PubMed\]](#)
4. Attia, H.; Meshreki, M.; Korashy, A.; Thomson, V.; Chung, V. Fretting wear characteristics of cold gas-dynamic sprayed aluminum alloys. *Tribol. Int.* **2011**, *44*, 1407–1416. [\[CrossRef\]](#)
5. Singh, J.; Lal, H.; Bala, N. Study of wear behaviour of HVOF and cold sprayed coatings on boiler steels. *Int. J. Mech. Eng. Robot. Res.* **2013**, *2*, 134–138.
6. Bolelli, G.; Lusvardi, L.; Barletta, M. Heat treatment effects on the corrosion resistance of some HVOF-sprayed metal alloy coatings. *Surf. Coat. Technol.* **2008**, *202*, 4839–4847. [\[CrossRef\]](#)
7. Papyrin, A.; Kosarev, V.; Klinkov, S.; Alkhimov, A.; Fomin, V.M. *Cold Spray Technology*, 1st ed.; Elsevier: Amsterdam, The Netherlands, 2007.
8. Manap, A.; Seo, D.; Ogawa, K. Characterization of thermally grown oxide on cold sprayed CoNiCrAlY bond coat in thermal barrier coating. *Mater. Sci. Forum* **2011**, *696*, 324–329. [\[CrossRef\]](#)
9. Manap, A.; Nooririnah, O.; Misran, H.; Okabe, T.; Ogawa, K. Experimental and SPH study of cold spray impact between similar and dissimilar metals. *Surf. Eng.* **2014**, *30*, 335–341. [\[CrossRef\]](#)
10. Schmidt, T.; Gärtner, F.; Assadi, H.; Kreye, H. Development of a generalized parameter window for cold spray deposition. *Acta Mater.* **2006**, *54*, 729–742. [\[CrossRef\]](#)
11. Manap, A.; Mahalingam, S.; Yusof, S.N.A.; Afandi, N.; Abdullah, H. Impact Behaviour of Aluminum Particles upon Aluminum, Magnesium, and Titanium Substrates using High Pressure and Low-Pressure Cold Spray. *Sains Malays.* **2022**, *51*, 585–597. [\[CrossRef\]](#)
12. Schmidt, T.; Assadi, H.; Gärtner, F.; Richter, H.; Stoltenhoff, T.; Kreye, H.; Klassen, T. From particle acceleration to impact and bonding in cold spraying. *J. Therm. Spray Technol.* **2009**, *18*, 794–808. [\[CrossRef\]](#)
13. Manap, A.; Ogawa, K.; Okabe, T. Numerical analysis of interfacial bonding of aluminum powder particle and aluminum substrate by cold spray technique using the SPH method. *J. Solid Mech. Mater. Eng.* **2012**, *6*, 241–250. [\[CrossRef\]](#)
14. Singh, H.; Sidhu, T.S.; Kalsi, S.B. Cold spray technology: Future of coating deposition processes. *Frat. Integrità Strutt.* **2012**, *22*, 69–84. [\[CrossRef\]](#)
15. Wang, Q.; Birbilis, N.; Zhang, M.X. Interfacial structure between particles in an aluminum deposit produced by cold spray. *Mater. Lett.* **2011**, *65*, 1576–1578. [\[CrossRef\]](#)
16. Yusof, S.N.A.; Manap, A.; Misran, H.; Othman, S.Z. Computational analysis of single and multiple impacts of low pressure and high pressure cold sprayed aluminum particles using SPH. *Adv. Mater. Res.* **2014**, *974*, 147–151. [\[CrossRef\]](#)
17. Yalcin, B. Effect of porosity on the mechanical properties and wear performance of 2% copper reinforced sintered steel used in shock absorber piston production. *J. Mater. Sci. Technol.* **2009**, *25*, 577–582.
18. Lee, H.; Shin, H.; Lee, S.; Ko, K. Effect of gas pressure on Al coatings by cold gas dynamic spray. *Mater. Lett.* **2008**, *62*, 1579–1581. [\[CrossRef\]](#)
19. Wang, Q.; Qiu, D.; Xiong, Y.; Birbilis, N.; Zhang, M.X. High resolution microstructure characterization of the interface between cold sprayed Al coating and Mg alloy substrate. *Appl. Surf. Sci.* **2014**, *289*, 366–369. [\[CrossRef\]](#)
20. Rokni, M.R.; Widener, C.A.; Crawford, G.A.; West, M.K. An investigation into microstructure and mechanical properties of cold sprayed 7075 Al deposition. *Mater. Sci. Eng. A* **2015**, *625*, 19–27. [\[CrossRef\]](#)
21. Marzbanrad, B.; Jahed, H.; Toyserkani, E. On the evolution of substrate's residual stress during cold spray process: A parametric study. *Mater. Des.* **2018**, *138*, 90–102. [\[CrossRef\]](#)

22. Koivuluoto, H.; Coleman, A.; Murray, K.; Kearns, M.; Vuoristo, P. High pressure cold sprayed (HPCS) and low pressure cold sprayed (LPCS) coatings prepared from OFHC Cu feedstock: Overview from powder characteristics to coating properties. *J. Therm. Spray Technol.* **2012**, *21*, 1065–1075. [[CrossRef](#)]
23. Ning, X.J.; Jang, J.H.; Kim, H.J.; Li, C.J.; Lee, C. Cold spraying of Al-Sn binary alloy: Coating characteristics and particle bonding features. *Surf. Coat. Technol.* **2008**, *202*, 1681–1687. [[CrossRef](#)]
24. Julio, V. Current and future applications of cold spray technology. *Met. Finish.* **2010**, *108*, 37–39.
25. Asuke, F.; Abdulwahab, M.; Aigbodion, V.S.; Fayomi, O.S.; Aponbiede, O. Effect of load on the wear behaviour of polypropylene/carbonized bone ash particulate composite. *Egypt. J. Basic Appl. Sci.* **2014**, *1*, 67–70. [[CrossRef](#)]
26. Stott, F.H. The role of oxidation in the wear of alloys. *Tribol. Int.* **1998**, *31*, 61–71. [[CrossRef](#)]
27. Manap, A.; Okabe, T.; Ogawa, K.; Mahalingam, S.; Abdullah, H. Experimental and smoothed particle hydrodynamics analysis of interfacial bonding between aluminum powder particles and aluminum substrate by cold spray technique. *Int. J. Adv. Manuf. Technol.* **2019**, *103*, 4519–4527. [[CrossRef](#)]